JOURNAL OF GEOPHYSICAL RESEARCH, VOL. 114, G03014, doi:10.1029/2008JG000942, 2009

Resazurin as a "smart" tracer for quantifying metabolically active transient storage in stream ecosystems

Roy Haggerty,[1] Eugènia Martí,[2] Alba Argerich,[3] Daniel von Schiller,[2,4] and Nancy B. Grimm[5]

Received 26 January 2009; revised 13 May 2009; accepted 11 June 2009; published 10 September 2009.

[1] We propose the experimental use of resazurin (Raz) and develop a metabolically active transient storage (MATS) model to include processes that may provide additional information on transient storage from a biogeochemical perspective in stream ecosystems. Raz is a phenoxazine compound that reduces irreversibly to resorufin (Rru) in the presence of aerobic bacteria. Raz was added as a stream tracer to a 128-m reach of the forested second-order Riera de Santa Fe del Montseny (Catalonia, NE Spain), along with a conservative tracer, NaCl. Raz was transformed to Rru at a rate of 0.81 h^{-1} in the hyporheic zone and only at a rate of 9.9×10^{-4} h^{-1} in the stream surface channel. Raz transformation and decay and Rru production and decay were both correlated with O_2 consumption measured at wells. The ratio of Raz to Rru concentration at the bottom of the reach was moderately correlated with instantaneous rates of net ecosystem production (NEP) measured over the whole reach. Data for Raz, Rru, and chloride were well fitted with the MATS model. The results from this study suggest that Raz transformation to Rru can be used as a ''smart'' tracer to detect metabolic activity, specifically aerobic respiration, associated with transient storage zones in stream ecosystems. Therefore, the Raz-Rru system can provide an assessment of the amount of transient storage that is metabolically active, an assessment that complements the physical characterization of transient storage obtained from conventional hydrologic tracers. The use of both physical and metabolic parameters of transient storage obtained with these tracers may increase our understanding of the relevance of transient storage on stream biogeochemical processes at whole reach scale, as well as the contribution of the different transient storage compartments to these processes.

Citation: Haggerty, R., E. Martí, A. Argerich, D. von Schiller, and N. B. Grimm (2009), Resazurin as a ''smart'' tracer for quantifying metabolically active transient storage in stream ecosystems, *J. Geophys. Res.*, *114*, G03014, doi:10.1029/2008JG000942.

1. Introduction

[2] Transient storage has become one of the most important concepts in hydrology and stream ecology in the past 25 years, helping to explain solute transport [*Bencala and Walters*, 1983; *Harvey and Bencala*, 1993; *Harvey et al.*, 1996], nutrient retention [*D'Angelo et al.*, 1993; *Valett et al.*, 1996], and heat transport in streams [*Johnson*, 2004; *Loheide and Gorelick*, 2006]. It is generated by the hydrological interaction between the surface stream and subsurface compartments, such as the hyporheic zone, and also by several different in-channel structures, such as pools, debris, and algal mats [*Harvey et al.*, 1996; *Gooseff et al.*, 2005]. This interaction may differentially influence stream biogeochemical processing based not only on water residence time but also on its biological and chemical properties [*Fisher et al.*, 1998; *McClain et al.*, 2003].

[3] Transient storage models (TSMs) generally include 1-D solute transport with source-sink term describing exchange [*Bencala and Walters*, 1983; *Harvey et al.*, 1996; *Runkel*, 1998; *Haggerty et al.*, 2002; *Wörman et al.*, 2002]. Parameters from TSMs characterize the relative size (A_s/A) of transient storage and its exchange rate (α) with free flowing water. These parameters have been widely used to examine the influence of transient storage on stream nutrient retention at whole reach scale [*Valett et al.*, 1997; *Mulholland et al.*, 1997; *Hall et al.*, 2002; *Thomas et al.*, 2003; *Webster et al.*, 2003; *Bukaveckas*, 2007; *Lautz and Siegel*, 2007; *Ryan et al.*, 2007]. Since transient storage zones have longer residence time than free flowing water, we expect greater

[1]Department of Geosciences, Oregon State University, Corvallis, Oregon, USA.
[2]Limnology Group, Centre d'Estudis Avançats de Blanes, Blanes, Spain.
[3]Departament d'Ecologia, Universitat de Barcelona, Barcelona, Spain.
[4]Now at Leibniz-Institute of Freshwater Ecology and Inland Fisheries, Berlin, Germany.
[5]School of Life Sciences, Faculty of Ecology, Evolution and Environmental Science, Arizona State University, Tempe, Arizona, USA.

0148-0227/09/2008JG000942$09.00

interaction between nutrients and organisms responsible for nutrient uptake in these zones; and thus, a relationship between transient storage parameters and nutrient retention. However, empirical relationships between transient storage and ecosystem processes are surprisingly weak or even contradictory [e.g., *Hall et al.*, 2002; *Webster et al.*, 2003; *Bukaveckas*, 2007]. This may stem from (1) the diversity of compartments that contribute to transient storage; (2) a true absence of relationship between transient storage zones and nutrient retention; and/or (3) the conservative tracer method commonly used to measure the TSM parameters does not allow evaluation of the biological nature or metabolic reactivity of the compartments that contribute to transient storage.

[4] We propose a metabolically active transient storage (MATS) model as a refinement of the TSM to focus on processes that are most relevant from a biogeochemical perspective. In its full form (to be described in a future paper), the MATS model would have separate compartments that distinguish transient storage zones with different levels of metabolism or, potentially, transient storage zones with different metabolic processes (e.g., autotrophic and heterotrophic metabolism, aerobic and anaerobic respiration). Similarly, some transient storage zones with different hydraulic properties (e.g., in-channel dead zones and hyporheic zones) may in some cases have similar metabolic function. In this paper, we will describe a simple MATS model wherein all transient storage zones have the same metabolism and hydraulic properties, and we use a tracer that is sensitive to aerobic respiration to parameterize that model.

[5] Resazurin (hereafter referred to as Raz) is a weakly fluorescent, nontoxic, redox-sensitive phenoxazine dye that undergoes an irreversible reduction to strongly fluorescent resorufin (hereafter referred to as Rru) under mildly reducing conditions, most commonly in the presence of aerobic respiration [*Karakashev et al.*, 2003]. The reduction of Raz to Rru is a well-documented indicator of the presence of living bacteria and is used in bacterial enumeration [*Liu*, 1983; *Peroni and Rossi*, 1986; *De Fries and Mistuhashi*, 1995; *O'Brien et al.*, 2000; *Guerin et al.*, 2001; *McNicholl et al.*, 2007] and toxicity tests [e.g., *Tizzard et al.*, 2006; *Mariscal et al.*, 2009]. *O'Brien et al.* [2000] reported that Raz reduction is insensitive to oxygen concentration but is very sensitive to microbial metabolism. *McNicholl et al.* [2007] showed that Raz reduction to Rru is proportional to aerobic respiration. In a laboratory study, *Haggerty et al.* [2008] characterized the decay, sorption, transformation, and transport of Raz and Rru in water and stream sediment. The study showed that Raz and Rru do not react or degrade in unfiltered stream water, but Raz transforms quickly (1.41 h^{-1}) to Rru in hyporheic sediment. Both Raz and Rru degrade in the light, but not sufficiently to pose a problem except in bright sunlight or over travel times of multiple hours in normal daylight. These results suggested that Raz could be a suitable tracer to help characterize transient storage from a metabolic perspective. *Haggerty et al.* [2008] refer to Raz as a "smart" tracer because, together with Rru, it provides information about processes other than transport (specifically, metabolism) in the environment through which it travels.

[6] The objectives of the present study were (a) to experimentally test the performance of Raz as a MATS-sensitive tracer under field conditions at the whole reach scale in a headwater stream; and (b) to develop a MATS model that includes Raz-Rru transformation and decay in both free flowing water and transient storage and test it against the field results.

2. Site Characterization

[7] The study was conducted in the Riera de Santa Fe, a perennial stream located at 1136 m above sea level in the Montseny Natural Protected Area (Catalonia, NE Spain; Figure 1). Monthly mean temperature ranges from 3°C in January to 20°C in August. Mean annual precipitation is approximately 1000 mm, occurring mostly as rain in autumn and spring but with occasional snow in winter. At the study site, the stream drains a 2.6-km^2 catchment forested primarily with silver fir (*Abies alba*) at higher elevations and beech (*Fagus sylvatica*) at lower elevations. Human use is mainly recreational, with some dispersed sheep grazing. A sample of sediment (<2 mm size fraction) collected from the streambed was silicic and consisted of 52.8% fine-grained metasedimentary lithic fragments, 34.8% quartz grains, 6.2% feldspar grains, 3.7% granodiorite lithic fragments, and 2.38 ± 0.18% (mean ± 2 SE) organic carbon. The bedrock is Cambrian-Ordovician shales and graywackes intruded by late Paleozoic biotite granodiorite [*Losantos et al.*, 2002].

[8] To perform the experiment, we selected a 128.3 m long, riffle-pool-dominated reach with a slope of 0.044 m m^{-1} (Figure 1; other physical parameters are provided in Table 1). A series of surface and subsurface sampling stations were distributed along the reach (Figure 1, see details in section 3). The streambed was composed of cobbles (47%), boulders (25%), and pebbles (21%), with patches of gravel and sand. Riparian vegetation was well developed and dominated by beech, with some common elder (*Sambucus nigra*) and a poorly developed herbaceous understory. The study was conducted in the spring (25 to 26 April) of 2007, a period characterized by moderate temperatures, near-constant flow conditions and relatively high light availability at the stream bottom because leaf emergence had not yet occurred. Previous studies in this reach have demonstrated high stream nutrient (phosphate and ammonium) retention efficiency with relatively high temporal variability associated with the interaction among the variation in stream discharge, water temperature and organic matter inputs [*Argerich et al.*, 2008; *von Schiller et al.*, 2008]. In this reach, the concentration of inorganic nutrients is usually low at this time of year [*von Schiller et al.*, 2008].

3. Methodology

3.1. Field Methods

[9] A 502-L solution containing 25.5 kg NaCl (hereafter "Cl") as a conservative tracer and 364.5 g of Raz was injected into the thalweg at the head of the reach using a Masterflex (Vernon Hills, Illinois) L/S battery-powered peristaltic pump at an initial rate of 400 mL min^{-1}. To correct results over time for changes in the injection rate, the voltage of the peristaltic pump was checked hourly using a digital multimeter. The experiment started at 1200 LT on 26 April and lasted 20 h. The injection rate was constant for 2 h and then declined approximately linearly by 1.78 mL min^{-1} h^{-1}, averaging 386 mL min^{-1} over the 20 h test. We

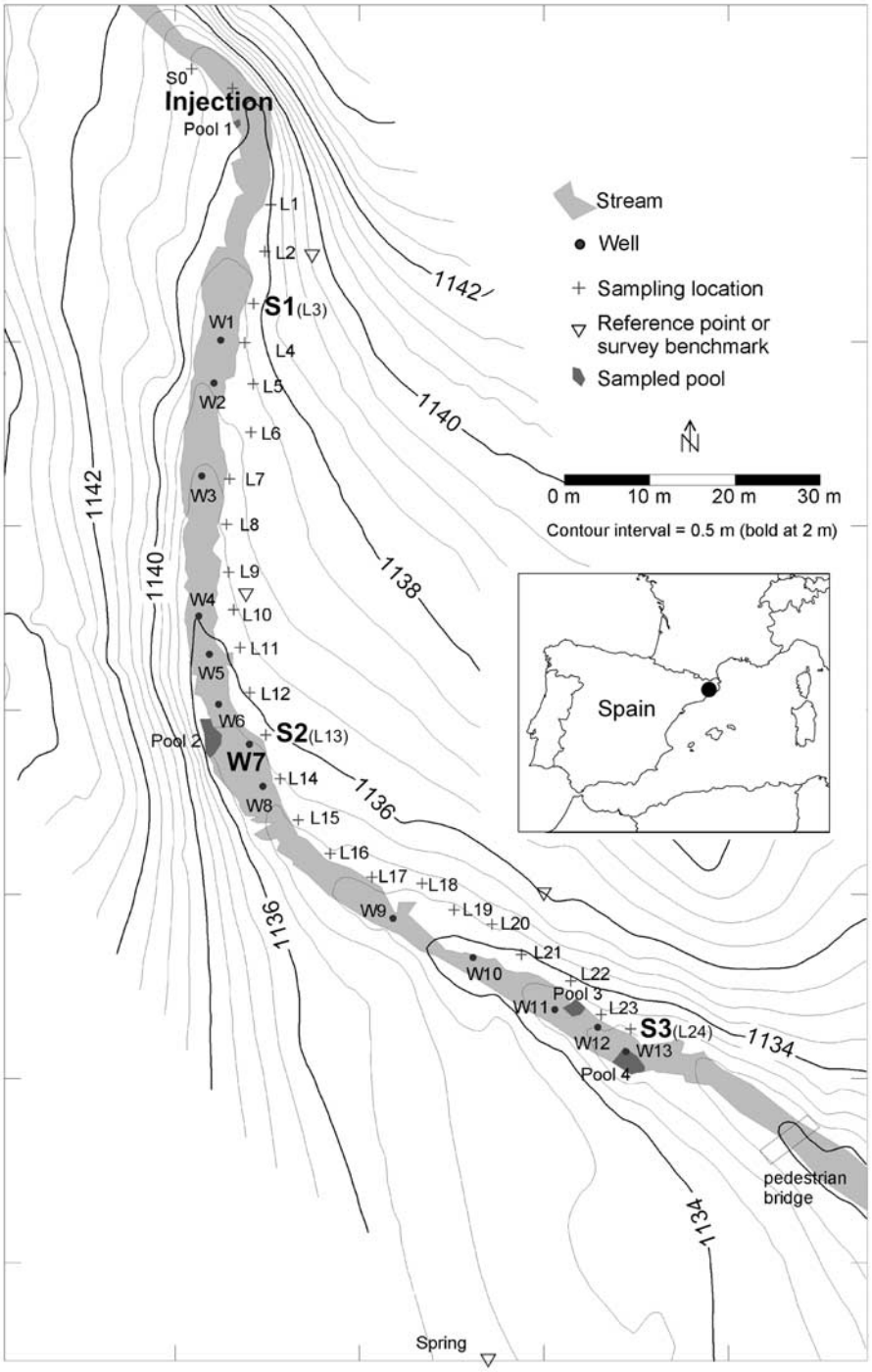

Figure 1. Map of the study reach in the Riera de Santa Fe del Montseny (Catalonia, NE Spain, 2°27′40″E, 41°46′ 34″N) where the tracers were injected. Number preceded by L indicates sampling sites (location stakes) for longitudinal variation of tracers in surface water, number preceded by S indicates sampling sites for temporal variation of tracers and O_2 in surface water, number preceded by W indicates well locations for sampling of tracers and O_2 in hyporheic water (W7 was also sampled in time), pool number indicates sampling sites for tracers in surface water pools. Contours are in m above sea level. Water surface elevation is shown in Figure 2.

used conductivity values as a surrogate for Cl concentrations to assess the changes due to the injection of the conservative tracer, and hereafter we refer to conductivity as Cl concentration. Chloride in surface stream water was automatically recorded every 5 s over the course of the experiment at three stations located at 24.7 m (S1), 74.3 m (S2), and 128.3 m (S3) from the injection point using a WTW (Weilheim, Germany) 340i portable conductivity meter connected to a CR510 Campbell Scientific (Logan, Utah) data logger. Four samples were taken from the carboy

Table 1. Physical and Chemical Characteristics and Daily Rates of Whole Reach Metabolism Measured in the Study Reach During the Experiment[a]

Physical Characteristics	Value	
Discharge (L s^{-1})	31.2 ± 0.07	
Width (m)	4.0 ± 0.4	
Depth (cm)	7.1 ± 0.7	
Temperature (°C)	9.5 ± 0.2	
PAR (mol m^{-2} d^{-1})	4.84	
Sunset 26 April 2007 (LT)	1843 (t = 6.72 h)	
Sunrise 27 April 2007 (LT)	0653 (t = 18.88 h)	
Chemical Characteristic	**Surface Water**	**Hyporheic Water**
Conductivity (μS cm^{-1})	44.5 ± 0.2	50.2 ± 1.3
Dissolved oxygen (mg L^{-1})	9.77 ± 0.03	7.2 ± 0.06
NO_3^- + NO_2^- (μg N L^{-1})	81 ± 8	95 ± 9
NH_4^+ (μg N L^{-1})	38 ± 7	84 ± 44
SRP (μg P L^{-1})	17 ± 4	35 ± 19
Metabolism	**Value**	
GPP (g O_2 m^{-2} d^{-1})	0.22	
ER (g O_2 m^{-2} d^{-1})	1.30	
GPP:ER	0.17	

[a]Chemical concentrations are immediately preinjection. Time in parentheses next to the sunset and sunrise indicate time since tracer injection started. Plus and minus values are 95% confidence intervals. PAR, photosynthetically active radiation. SRP, soluble reactive phosphorus. GPP, gross primary production; and ER, ecosystem respiration.

solution at different times during the injection experiment, and one additional sample was collected from the solution remaining after the completion of the experiment to measure concentration of Raz, Rru, and Cl in the added solution.

[10] We defined a total of 28 surface water sampling points distributed along the reach (4 located in pools and the rest in the thalweg; Figure 1). Pools were sampled because of their in-channel hydraulic retention. We also installed 13 PVC wells (a mixture of 22 mm and 26 mm ID; W7 was 22 mm ID) to a depth of 21.4 ± 21.6 cm (maximum 35.8 cm, minimum 4.8 cm) below the streambed to collect subsurface water samples along the reach (Figure 1). To characterize the longitudinal concentration profile of the tracers in the surface and subsurface water, we measured conductivity and collected water samples from all sampling points before the experimental addition started and at two times during plateau conditions: t = 7 h (1900 LT) to capture end-of-day conditions, and t = 18 h (0600 LT) to capture end-of-night conditions. Sunset and sunrise were at tracer injection times 6.72 and 18.88 h, respectively. Two surface stations (S2 and S3) and one well station (W7, colocated at S2, depth of 35.8 cm, the deepest well) were sampled hourly during the experiment to monitor changes in tracer concentration over time. Prior to each well sample, approximately 40% of the well volume was purged, followed by a sample of approximately 20% of the well volume. Also, at S2, we conducted an intensive sampling every 20 min during the first 2 h of the experiment and every 5 min after the injection of solute was stopped, to detail the rising and falling limbs of the breakthrough curve. Additional water samples from a subset of surface water stations and from all the wells were collected before the injection and at the two plateau samplings for the analysis of nitrate + nitrite (NO_3^- + NO_2^-), ammonium (NH_4^+) and soluble reactive phosphorus (SRP) concentrations.

[11] Additionally, we placed a set of 78 μg L^{-1} Raz and 24 μg L^{-1} Rru standards in the dark (spikes) and another set was placed in glass scintillation vials in the stream to be exposed to ambient light. Samples from the two sets of standards were collected hourly (n = 22 for each Raz and Rru, light and dark), simultaneous with sampling at S2, S3 and W7, and processed with the rest of samples to monitor photodegradation and other systematic errors during the experiment. All samples for Raz and Rru determination were immediately filtered through Whatman (Kent, United Kingdom) GF/F glass fiber filters (0.7 μm pore size), placed in glass scintillation vials, stored on ice in the dark, and refrigerated at 4°C in the laboratory until analysis.

[12] Stage was automatically recorded every 5 min using a CS-420-L submersible pressure transducer (Campbell Scientific) connected to a CR510 Campbell Scientific data logger at S1. Average reach width and depth were calculated as the mean of measurements made on cross-sectional transects at each sampling point. Vertical hydraulic gradient (VHG) was measured in each well following the methodology described by *Dahm et al.* [2006].

[13] Whole reach metabolism was estimated using the upstream-downstream diurnal dissolved oxygen (O_2) change technique [*Bott*, 2006]. Dissolved O_2 concentration and temperature were recorded at two stations (S1 and S3) at 10-min intervals during a 24-h period (starting at 1000 LT, 25 April) with a WTW (Weilheim, Germany) 340i portable oxygen meter. Measurements were done simultaneously with the injection experiment. Percent O_2 saturation was estimated using O_2 concentration and temperature data together with a standard altitude-air pressure algorithm to correct for site altitude. Additionally, O_2 concentration was measured in each well during the two longitudinal sampling times. We estimated daily rates of gross primary production (GPP, g O_2 m^{-2} d^{-1}) and ecosystem respiration (ER, g O_2 m^{-2} d^{-1}) by integrating the net rate of O_2 change (corrected for reaeration flux) between the two stations over the 24-h period following *Bott* [2006]. Exchange of O_2 with the atmosphere (i.e., reaeration flux) was calculated based on the average O_2 saturation deficit in the reach, the reaeration rate, the travel time between the two stations, and the stream discharge. The reaeration rate (0.081 min^{-1}) was estimated based on the nighttime regression method [*Young and Huryn*, 1996]. ER was calculated as the average corrected net nighttime O_2 change rate extrapolated to 24 h. GPP was computed by integrating the difference between the corrected net O_2 change rates and the extrapolated daytime respiration rates. GPP and ER rates were expressed per unit of reach surface area (i.e., distance between the two stations times the average wetted width).

[14] The stream was surveyed on 28 and 30 May 2007 using a Geodimeter 506b (now owned by Trimble, Sunnyvale, California) total station (Figure 1). Stream discharge was not measured during the survey, but was visually similar to that observed during the tracer experiment one month earlier. Stream left and right were shot at every point that differed by more than approximately 5 cm vertically from any adjacent point. We recorded the locations of all wells, all stakes marking sample locations, and several dozen topographic points adjacent to the stream. The water surface slope (Figure 2) of the reach was nearly uniform, with a few exceptions just downstream of the injection site, downstream of S2, and upstream of S3. Relatively strong

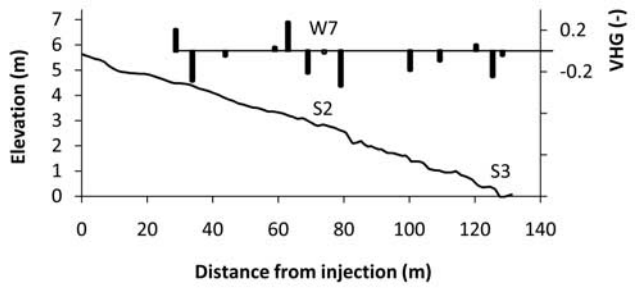

Figure 2. Water surface elevation of centerline of stream (elevation relative to surface sampling location S3) and vertical hydraulic gradient (VHG) in the wells.

downwelling appeared upstream of the higher gradient in water surface elevations near S2 and S3.

3.2. Laboratory Methods and Metabolism Calculation

[15] All reagents were purchased from Panreac Química S.A. (Castellar del Vallès, Barcelona, Spain; http://www.panreac.com) and used as supplied. Comparison of fluorescence signals showed that Raz was contaminated by 3.1% Rru. Raz and Rru have constant fluorescence above approximately pH 8, but have decreasing fluorescence at lower pH [*Kangasniemi*, 2004; *Bueno et al.*, 2002]. We would like to note that this is only a lab measurement issue because it has no effect on transformation, decay or other field processes. Consequently, water samples from the experiments were buffered to pH 8 prior to analysis of Raz and Rru. A stock solution of buffer near pH 8.0 was generated by mixing 1 M $NaH_2PO_4 \cdot H_2O$ with equal parts of 1 M NaOH. The solution was added to samples at a 1:10 buffer-to-sample ratio immediately before fluorescence measurement. All laboratory materials were triple washed with tap water, triple rinsed with deionized water, and air-dried if needed. Fluorescence of Raz and Rru in water samples was measured on a Shimadzu (Kyoto, Japan) RF spectrofluorometer, with excitation and emission wavelengths given by *Haggerty et al.* [2008]. Samples were placed in a quartz cuvette and held within the sample chamber for less than 1 min to minimize temperature changes. Samples were analyzed within 72 h of the experiment. The limit of quantization (LOQ) for Raz and Rru in natural water measured with this instrument were 0.8 μg L^{-1} and 0.06 μg L^{-1}, respectively [*Haggerty et al.*, 2008]. Analysis of field spikes and blanks indicates the 95% confidence interval on Raz is ±8.4% of concentrations and the 95% confidence interval on Rru is ±5.7% of concentrations. Confidence bounds grow relatively larger for small concentrations near the LOQ. Concentrations of NO_3^- + NO_2^-, NH_4^+ and SRP in stream water samples were analyzed with a Bran + Luebbe (Norderstedt, Germany) TRAACS 2000 Autoanalyzer following standard colorimetric methods [*Clesceri et al.*, 1999].

[16] The fraction of tracer-labeled surface water (%SW) present in wells was calculated by comparing the background-corrected conductivity in the well and adjacent surface water. We calculated the expected Raz concentration in wells in the absence of transformation or decay by multiplying the %SW in the well by the Raz concentration measured at the surface. Similarly, we calculated the expected Rru concentration in wells in the absence of transformation or decay by following the same procedure as for Raz concentration. These expected values were compared to observed concentrations to evaluate Raz and Rru gains or losses in the wells relative to what was expected by hydrologic exchange alone.

3.3. Modeling

[17] The stream transport, dispersion, transformation, decay and transient storage exchange of Raz, Rru, and Cl were modeled using a coupled 1-D model. The model was similar to that given by *Bencala and Walters* [1983], *Harvey et al.* [1996], and *Runkel* [1998, 2007] which assumes an exponential residence time distribution (RTD) in storage zones. However, here it was modified for coupled, three-component transport (one conservative and two nonconservative tracers). Although complete exposition is beyond the scope of this paper, we eventually intend for the model to incorporate a discrete number of MATS zones with different rates of metabolism. For clarity, the most important processes are described in parentheses after each equation; furthermore the equations are given in the same order as the dominant pathway for Raz to Rru transformation and transport.

$$\frac{\partial C_{Raz}}{\partial t} = -\frac{Q}{A}\frac{\partial C_{Raz}}{\partial x} + \frac{1}{A}\frac{\partial}{\partial x}\left(AD\frac{\partial C_{Raz}}{\partial x}\right) - \frac{R_s A_s}{A}(C_{Raz} - S_{Raz}) - \left(k_1^c + k_{12}^c\right)C_{Raz} \quad (1)$$

(Key processes are Raz transport in surface channel with transfer to the MATS zone.)

$$\frac{\partial S_{Raz}}{\partial t} = \frac{1}{t_s R_s}(C_{Raz} - S_{Raz}) - \left(k_1^s + k_{12}^s\right)S_{Raz} \quad (2)$$

(Key processes are Raz variation in MATS zone due to transfer from surface stream, decay loss, and transformation to Rru in the MATS zone.)

$$\frac{\partial S_{Rru}}{\partial t} = \frac{1}{t_s R_s}(C_{Rru} - S_{Rru}) - k_2^s S_{Rru} + k_{12}^s \frac{M_{Rru}}{M_{Raz}} S_{Raz} \quad (3)$$

(Key processes are Rru variation in MATS zone due to transfer to surface stream, decay loss, and transformation from Raz in the MATS zone.)

$$\frac{\partial C_{Rru}}{\partial t} = -\frac{Q}{A}\frac{\partial C_{Rru}}{\partial x} + \frac{1}{A}\frac{\partial}{\partial x}\left(AD\frac{\partial C_{Rru}}{\partial x}\right) - \frac{R_s A_s}{A}(C_{Rru} - S_{Rru}) - k_2^c C_{Rru} + k_{12}^c \frac{M_{Rru}}{M_{Raz}} C_{Raz} \quad (4)$$

(Key processes are Rru transport in surface channel with transfer from the MATS zone.)

[18] Variables and parameters are defined in the notation section. Cl transport is modeled with equations (1) and (2) but with no transformation, decay and retardation factor, i.e., the model for Cl is the TSM [e.g., *Runkel*, 2007]. Note that $t_s = A_s/(A\alpha)$.

[19] Boundary conditions were a 20-h injection of constant concentration at $x = 0$ preceded and proceeded by zero

Table 2. Parameter Values for Model Shown in Figure 3[a]

Parameter	Value[b]
Velocity (v, m h^{-1})	509
A_s/A	0.76
Dispersion coefficient in stream (D, m^2 s^{-1})	1.07
Mean residence time in MATS zone (t_s, h)	1.56
Retardation factor in transient storage zone for Raz and Rru	2.50

Raz and Rru Reaction Rates	Channel	Transient Storage Zone
Raz decay (k_1, h^{-1})	0	0.22
Raz to Rru transformation (k_{12}, h^{-1})	9.9×10^{-4}	0.81[b]
Rru decay (k_2, h^{-1})	1.8×10^{-3}	1.6

[a]Channel reaction rates were measured in the lab by *Haggerty et al.* [2008]; k_1^s and k_2^s (transient storage zone decay rates) were measured relative to k_{12}^s from the well data in Figure 7.
[b]Parameter values estimated from the data in Figure 3.

concentration, and a downstream boundary of zero concentration at $x \rightarrow \infty$. Concentration of Cl during the injection experiment (after subtracting background) was normalized to that of injected Raz for presentation purposes. Injection concentration of Rru was 3.1% of Raz. Initial conditions for Raz, Rru, and background-subtracted Cl were 0 everywhere.

[20] Equations (1)–(4) along with boundary and initial conditions were transformed into the Laplace domain and solved. We used a numerical inversion from the Laplace domain to obtain time domain results. Finally, the time domain solution was wrapped within a Levenberg-Marquardt algorithm [*Marquardt*, 1963] to provide parameter estimation. The solution technique and code is similar in overview to STAMMT-L [*Haggerty and Reeves*, 2002] and will be upgraded and released as STAMMT-L 3.0. The code was validated mathematically against two analytical solutions, one for first-order mass transfer with a single component [*Toride et al.*, 1995], and one for diffusive mass transfer and transport with multiple compounds [*Sun and Buscheck*, 2003]. More details on the model will be provided in a forthcoming paper.

[21] The model, as shown, assumes an exponential MATS zone RTD. We have developed and implemented a multirate model [*Haggerty and Gorelick*, 1995; *Haggerty et al.*, 2002; *Wörman et al.*, 2002] that relaxes the exponential RTD (e.g., could be lognormal or power law), but we have not used the multirate model in the current application. The model assumes that the different compartments contributing to transient storage all have the same transformation and decay rates, an assumption that is probably unrealistic given what is known about likely sites of surface and subsurface storage. The model further assumes that the transformation and decay rates are constant in time. This assumption is valid because most of the reaction probably happens in the subsurface, where temperature does not change much over a day.

[22] A single model, the solution to equations (1)–(4), was generated for all surface water Cl, Raz and Rru concentrations varying both in space along the reach and in time over the course of the injection. Transformation and decay rates for surface water (k_1^c, k_{12}^c, and k_2^c) in this stream were measured and reported by *Haggerty et al.* [2008]. The transformation rate of Raz to Rru in the MATS zones (k_{12}^s) was estimated with the model from the field experimental data, and k_1^s and k_2^s were fixed by ratios relative to respiration estimated from the well data (see below). Velocity, dispersion, A_s/A, and t_s were estimated simultaneously from surface concentrations of Raz, Rru and Cl. Values of all model parameters except the retardation factor were the same for Raz, Rru, and Cl (Table 2).

[23] Uptake length, S_w [*Stream Solute Workshop*, 1990], for Raz was calculated according to *Runkel* [2007, equation 12] taking proper account of stream transport, from the stream discharge and the transport model parameters α, k_{1Tot}^c [T^{-1}] (the sum of k_1^c and k_{12}^c), k_{1Tot}^s [T^{-1}] (the sum of k_1^s and k_{12}^s), R_s, and A_s/A. Uptake velocity, V_f, was calculated from these parameters and average water depth in the stream.

[24] Dissolved O_2 concentrations were related to Raz and Rru concentrations in the hyporheic zone by first assuming that O_2 is consumed according to a first-order law. The O_2 fraction, F_{O_2} [dimensionless], is the O_2 concentration in the well divided by the O_2 concentration that entered the hyporheic zone from the surface stream. Similarly, F_{Raz} is the Raz fraction and F_{Rru} is the Rru fraction (see the notation section for definitions). In all cases, the fractions were normalized by percent surface water (%SW) in the wells, which assumes that groundwater has concentrations of 0 for each solute, a valid assumption for Raz and Rru but less certain for O_2. After normalizing for %SW, and neglecting hyporheic zone dispersion,

$$F_{O_2} = \exp\left[-k_{O_2}^s \tau\right] \tag{5a}$$

This can be rearranged as

$$\tau = -\frac{\ln(F_{O_2})}{k_{O_2}^s} \tag{5b}$$

For plateau conditions, (5b) can be substituted into a first-order expression for Raz, similar to (5a), and F_{Raz} has an algebraic (power law) relationship to F_{O_2} as follows:

$$F_{Raz} = \exp\left[\frac{k_{1Tot}^s}{k_{O_2}^s}\ln(F_{O_2})\right] = F_{O_2}^{k_{1Tot}^s/k_{O_2}^s} \tag{6}$$

F_{Rru} is expressed as follows on the basis of the work by *Haggerty et al.* [2008]:

$$F_{Rru} = \frac{C_{Raz}M_{Rru}}{C_{Rru}M_{Raz}}\frac{k_{12}^s}{k_2^s - k_{1Tot}^s}\left[\exp\left(-k_{1Tot}^s t\right) - \exp\left(-k_2^s t\right)\right] + \exp\left(-k_2^s t\right) \tag{7}$$

where C_{Raz} and C_{Rru} are the concentrations in the surface stream as previously defined, at plateau. Substituting (5b) into (7), we also get an algebraic relationship between F_{Rru} and F_{O_2}:

$$F_{Rru} = \frac{C_{Raz}M_{Rru}}{C_{Rru}M_{Raz}}\frac{k_{12}^s}{k_2^s - k_{1Tot}^s}\left(F_{O_2}^{k_{1Tot}^s/k_{O_2}^s} - F_{O_2}^{k_{1Tot}^s/k_{O_2}^s}\right) + F_{O_2}^{k_2^s/k_{O_2}^s} \tag{8}$$

Equations (6) and (8) allow us to estimate the magnitudes of k_1^s, k_{12}^s, and k_2^s relative to $k_{O_2}^s$ from fractions of O_2, Raz, and

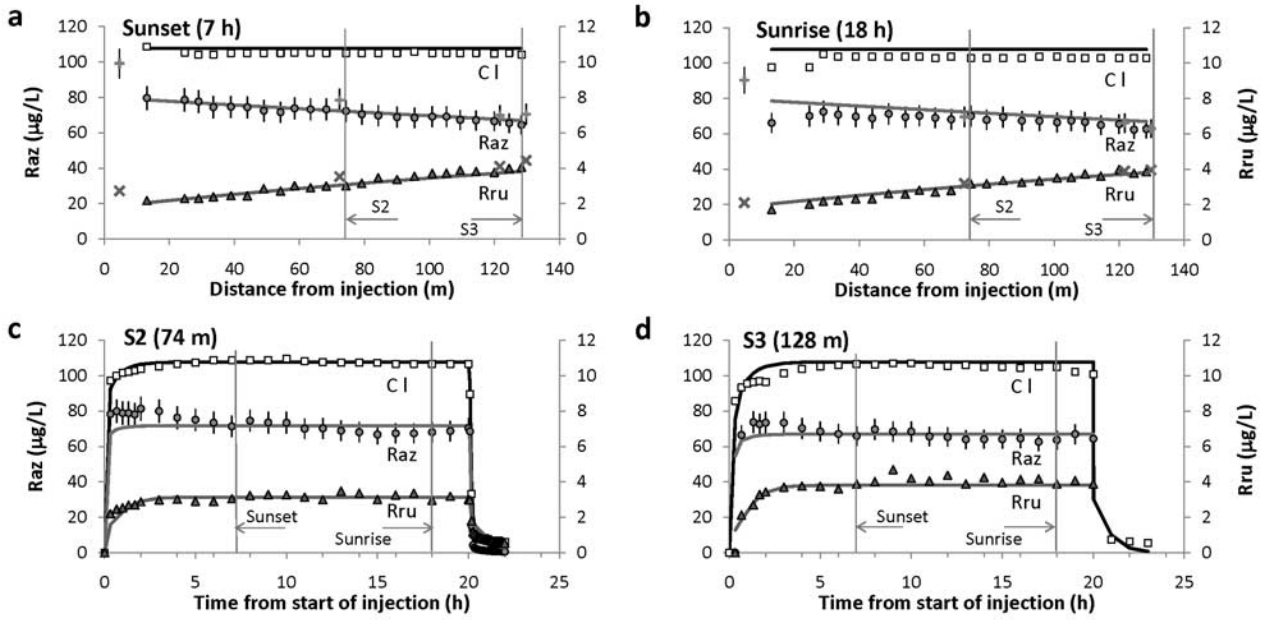

Figure 3. Measured and modeled concentrations of resazurin (Raz) and resorufin (Rru) in surface water from the whole reach tracer injection in the Riera de Santa Fe. (a and b) Concentration profiles along the reach at 7 and 18 h of tracer injection. (c and d) Breakthrough curves at S2 (74.3 m) and S3 (128.3 m). Pluses and crosses in Figures 3a and 3b indicate surface water concentrations in pools. Vertical lines in Figures 3a and 3b indicate sample locations for breakthrough curves (BTCs). Vertical lines in Figures 3c and 3d indicate sampling time for longitudinal samples. Concentrations of Cl are rescaled to expected Raz injection concentration of 107.7 μg L^{-1}. Error bars show 95% confidence bounds. Where no error bars are shown, 95% confidence bounds are smaller than symbol. Solid lines behind data are results from a model of transport, advection, dispersion, transient storage, and transformation and decay in both channel and transient storage zone, with a single set of parameters (see text for details). The root-mean-square error (RMSE) of the model is 4.38 μg L^{-1}; the RMSE at plateau alone is 2.75 μg L^{-1}.

Rru. On the basis of these equations, in any hyporheic zone, F_{Raz} will start at 1 and decrease monotonically to zero with decreasing F_{O_2}. In the same hyporheic zone, F_{Rru} will start at 1, initially will increase, will peak, and then will decrease to zero with decreasing F_{O_2}. Equations (6) and (8) can be written without neglecting hyporheic zone dispersion but are more complicated and do not change results much; furthermore, dispersion is usually poorly constrained in the hyporheic zone.

[25] We fit the relationships in (6) and (8) to well data to determine the ratios $k_1^s/k_{O_2}^s$, $k_{12}^s/k_{O_2}^s$, and $k_2^s/k_{O_2}^s$. Once these ratios are known, the resulting ratio of rate coefficients k_1^s: k_{12}^s: k_2^s is known. This ratio of rate coefficients was fixed in the transport modeling, allowing us to estimate only one rate coefficient (k_{12}^s). The other rate coefficients are then calculated using the ratio.

4. Results

4.1. Surface Water Results

[26] Discharge during the experiment was 31.2 ± 1.2 L s^{-1} (Table 1). We were fortunate to have discharge drop at almost exactly the same rate as the injection, and so after mixing with stream water, the injected concentrations were very nearly constant in time. Surface water presented higher dissolved O_2 concentration but lower tracer and nutrient concentrations than hyporheic water (Table 1).

[27] Longitudinal profiles of Cl concentration were steady with travel distance and similar for the two plateau samplings (Figures 3a and 3b). Cl concentration within <25 m from the injection site showed discordant values due to insufficient mixing. This was also observed for Raz and, to a lesser extent, for Rru concentrations. Concentration of Raz decreased and that of Rru increased consistently with travel distance in both plateau samplings (Figures 3a and 3b). However, there were some differences between the two sampling times. The ratio of Raz to Cl along the reach was slightly higher (two-sided t test on detrended values, $p < 0.001$) at the sunset sampling (average Raz/Cl = 0.68 ± 0.07) than at the sunrise sampling (average Raz/Cl = 0.66 ± 0.05). Similarly, the ratio of Rru to Cl along the reach was also slightly higher (two-sided t test on detrended values, $p < 0.001$) at the sunset sampling (average Rru/Cl = 0.030 ± 0.012) than at the sunrise sampling (average Rru/Cl = 0.029 ± 0.012). Longitudinal concentration profiles indicated pseudo-first-order conversion of Raz to Rru. The sum of Raz and Rru indicated that there was a 15% mass loss over the reach. Longitudinal changes of Raz and Rru surface concentrations were uncorrelated with either changes in water surface elevations or VHG values measured in the wells (Figure 2).

[28] Raz and Rru surface concentrations in pools at the first sampling plateau were higher than concentrations in adjacent thalweg surface water (Figure 3a). Ignoring pool 1 (which may not have been well mixed because of proximity to the injection

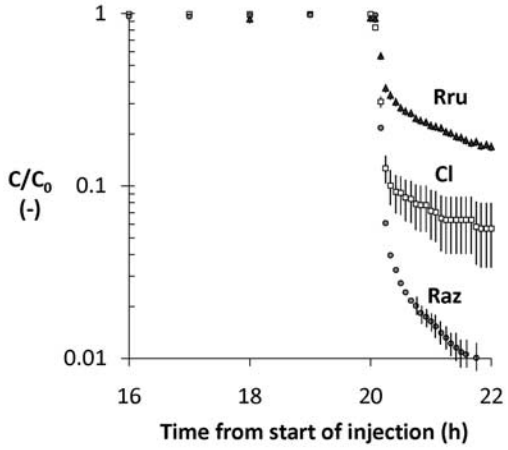

Figure 4. Tail of the breakthrough curves for resazurin (Raz), resorufin (Rru), and chloride (Cl) at sampling station S2 (74.3 m from injection point). For comparison, the concentration (C) of each compound was divided by the plateau concentration (C_O) and data are shown with a logarithmic scale. Tracer injection was stopped at 20 h. Error bars are shown where the 95% confidence bounds are larger than the symbol.

and which had no adjacent thalweg sampling point), Raz concentration was 5.3 μg L^{-1} and Rru concentration 0.3 μg L^{-1} higher in the pools than in adjacent surface water at the first plateau sampling (two-sided t test on detrended data, $p < 0.001$ in both cases). Conversely, no concentration differences between pools and adjacent surface water were found at the second plateau sampling (two-sided t test on detrended data, $p > 0.1$ in both cases). Unfortunately, we neglected to take pool samples for Cl, so we were not able to check if a similar pattern was present for the conservative tracer.

[29] Breakthrough curves (BTCs) showed distinct behavior for Raz, Rru, and Cl (Figures 3c, 3d, and 4). The BTC for Cl was typical for streams with a moderate transient storage zone, displaying an initial rapid rise, a shoulder, a broad steady plateau, an initial rapidly falling tail, and a small extended tail (Figures 3c, 3d, and 4). The BTC for Raz showed a much sharper rise and fall with no shoulder and almost no tail (Figure 4). Finally, the Rru BTC rose more slowly than the BTCs for both Cl and Raz, taking several hours to reach plateau. The Rru tail was extensive; 2 h postinjection, Rru concentration was still 17% of the plateau concentration and more than 50% of early tail concentration (20 min postinjection). Raz and Rru BTCs at plateau showed some temporal variation over the duration of the injection. Raz concentration at plateau was highest shortly after the injection started, when daylight was highest, and decreased until approximately sunset. During the same period, Rru was approximately at plateau in the hours before sunset and increased slightly after sunset.

[30] The field standards placed in the light showed a decrease of Rru but not of Raz concentration during the experiment. This was likely due to phodegradation because the decrease was only significant during daylight hours (Pearson's correlation, $p = 0.004$, $r^2 = 0.67$, $n = 10$), and was not significant during nighttime hours (Pearson's correlation, $p = 0.176$, $r^2 = 0.18$, $n = 12$). The first-order degradation rate for Rru was 0.27 h^{-1} for the first 3 h of the experiment, when light was maximal. The photodegradation effect was probably diminished by the glass bottles, however, because glass filters a high proportion of UV light. Nevertheless, the effect of photodegradation was likely negligible due to the short water traveling time (0.25 h from injection to S3) and because the first 3 h of the experiment were the least important for our results.

[31] The daily rate of whole reach metabolism was dominated by respiration (GPP:ER = 0.17; Table 1). However, stream metabolism varied over the course of the day, with maximum GPP at 1000 LT ($\sim$1.5 mg m^{-2} min^{-1}) and a mean ER of $\sim$0.9 mg m^{-2} min^{-1}. Instantaneous rates of net ecosystem production (NEP) therefore were highest 2 h prior to the start of the experiment and declined to a low (equal to ER) during the nighttime (Figure 5). The ratio of concen-

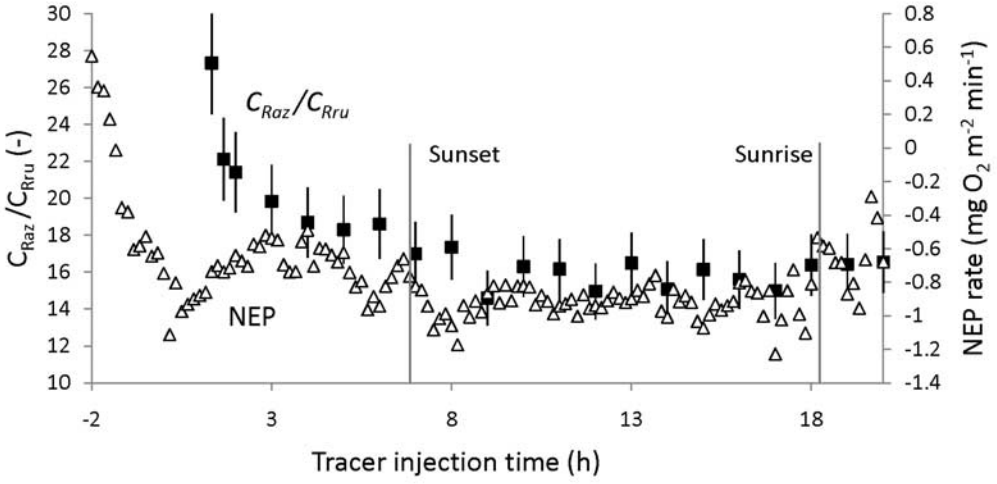

Figure 5. Temporal variation over the duration of the tracer injection of the resazurin/resorufin concentration ratio (solid squares) and the instantaneous rate of net ecosystem production (NEP, open triangles). Raz and Rru concentrations are from surface water at S3. NEP rate was calculated from S1 and S3 (see section 3.1).

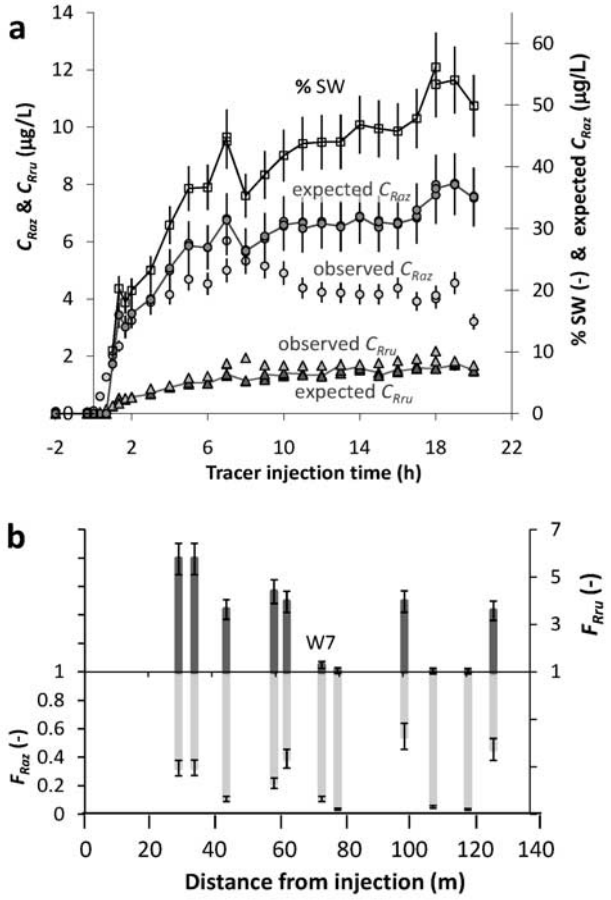

Figure 6. Results for tracers measured in the wells. (a) Breakthrough curves measured in W7 (colocated with surface sampling point S2) showing the percentage of surface water (%SW, as measured by Cl) and the observed and expected (based on %SW) concentrations of resazurin (Raz) and resorufin (Rru). Higher expected than observed concentrations indicate a loss of tracer in the subsurface, whereas lower expected than observed concentrations indicate production of tracer in the subsurface. (b) Spatial variation of the fraction of surface water Raz (F_{Raz}) and Rru (F_{Rru}) among the sampling wells located along the reach measured at tracer injection time 18 h (i.e., the second plateau sampling). Values less than 1 indicate tracer loss (observed for Raz at all wells), and values greater than 1 indicate tracer production (observed for Rru at all wells). W6 and W12 were not sampled at 18 h because of insufficient flow for required purge and sample volumes.

trations of Raz and Rru at plateau provides an index of biological activity in storage zones, i.e., an index of MATS. Accordingly, a correlation between NEP and C_{Raz}:C_{Rru} (Figure 5; the Pearson product-moment correlation coefficient is $r = 0.476$ ($p < 0.05$) and Spearman's rank correlation coefficient is $r_s = 0.631$ ($p < 0.005$)) at plateau ($t \geq 3$ h) indicated that lower values of NEP (i.e., higher ER) were associated with the transformation of Raz to Rru.

4.2. Hyporheic Results

[32] Results from Cl data in W7 indicated that surface water reached this subsurface location within an hour of the start of the tracer injection (Figure 6a). The %SW in this well gradually increased during the experiment, reaching ~50% by the end of the sampling (i.e., at 20 h; Figure 6a). However, tracer concentration did not reach a clear plateau in the well. If we assume that plateau occurred at ~50% surface water, the nominal travel time to the well was approximately 3.2 h. Conversely, concentrations of Raz and Rru in the well gradually increased within the first 8 h of injection and then appeared to reach a plateau. Raz concentrations observed in the well from 5 to 20 h were much lower (two-sided t test, $p < 0.001$) than those expected in the absence of transformation or decay (Figure 6a). Rru concentrations observed in the well from 5 to 20 h (mean 1.7 ± 0.4 µg L^{-1}) were higher (two-sided t test, $p < 0.001$) than those expected in the absence of gains from transformation (mean 1.4 ± 0.4 µg L^{-1}; Figure 6a). However, gains of Rru did not fully account for losses of Raz; that is, additional losses of either Raz or Rru (or both) were required to fully explain the data.

[33] Values of Cl concentration, F_{Raz}, and F_{Rru} measured in the remaining wells (Figure 6b) at the second surface water plateau (sunrise) also showed surface-to-subsurface water exchange. Despite variability among wells, lower Raz ($F_{Raz} < 1$) and higher Rru ($F_{Rru} > 1$) concentrations than expected without transformation or decay were consistent with patterns in W7.

[34] Dissolved O_2 concentrations were lower in the wells than in surface water (i.e., $F_{O_2} < 1$ in Figure 7) and variability among wells in the fraction of Raz and Rru was correlated with the model value based on F_{O_2} ($r^2 = 0.81$ and 0.65, respectively, both $p < 0.001$). F_{Raz} generally dropped with F_{O_2}, suggesting a correlation of Raz decay and transformation due to aerobic respiration. F_{Rru} at first rose with falling F_{O_2} and then dropped. The fits of (6) and (8) to the Figure 7 data yielded $k_1^s/k_{O_2} = 1.22$, $k_{12}^s/k_{O_2}^s = 4.44$, and $k_2^s/k_{O_2}^s = 8.61$. Field results were consistent with the lab results [*Haggerty et al.*, 2008] except that transformation and decay rates were lower in the lab ($k_1^s/k_{O_2}^s = 0.35$, $k_{12}^s/k_{O_2}^s = 3.49$, and $k_2^s/k_{O_2}^s = 1.27$. The value of $k_{O_2}^s$ was 0.18 h^{-1} in the hyporheic zone during the experiment, calculated from the above ratios and rate coefficients estimated by the model (section 4.3; Table 2).

4.3. Modeling Results

[35] The model captured the major features of the longitudinal concentration profiles and BTCs for all the tracers, and was consistent with both the surface and the subsurface data. Modeled longitudinal concentration profiles generally agreed well with the data, although with slightly different slopes, possibly indicating an error in upstream concentrations (Figures 3a and 3b). Modeled arrival of tracer, the shoulder of the rising limb of the BTC, and plateau concentrations of all three tracers were very similar to the data (Figures 3c and 3d). Modeled tails of the BTC were similar to the data, Rru, Cl, and Raz concentrations were ordered properly and agreed with measured concentrations, although the shape of the tail of the model was slightly different than that of the data (not shown in detail). Estimated parameters

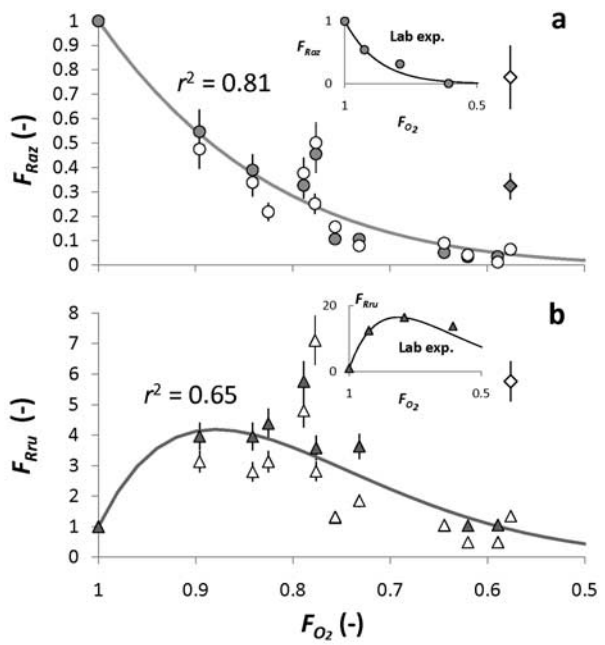

Figure 7. Relationships between fraction of surface water Raz (F_{Raz}) and Rru (F_{Rru}) found in each of the wells versus fraction of surface water O_2 (F_{O_2}) found in each of the wells. Open symbols correspond to data collected at $t = 7$ h (sunset), and filled symbols correspond to data collected at $t = 18$ h (sunrise). Inset graphs show lab experiments from *Haggerty et al.* [2008, Table 1b], where fraction was calculated from outlet/inlet for a column. Diamonds indicate values at W1, which were thrown out of r^2 calculation because the stream was not well mixed at this point. The model fit to the well data produced the ratios k_1^s:k_{12}^s and k_2^s:k_{12}^s that were used in the model shown in Figure 3.

(Table 2) were reasonable and self-consistent. Together, these facts indicate that our mathematical description of the Raz reduction to Rru and transport were broadly accurate.

5. Discussion

[36] The results of the field injection suggest the intriguing possibility of using Raz as a "smart" tracer to investigate spatial and temporal patterns of MATS at the subreach to reach scale. The study found a correlation between Raz transformation to Rru and oxygen consumption (wells, Figure 7) and instantaneous rates of NEP in surface water (Figure 5) in this heterotrophic stream. The findings are consistent with the well-documented result that living bacteria, particularly aerobic bacteria [*Karakashev et al.*, 2003], transform Raz to Rru, and are consistent with the lab result that Raz reduction is proportional to aerobic respiration [*McNicholl et al.*, 2007]. Our results suggest that the Raz to Rru transformation is correlated with aerobic respiration in the field. Furthermore, the study of *Haggerty et al.* [2008] showed that the Raz to Rru transformation is negligible in the water column but rapid in sediment. Together, these results indicate that Raz may be used to trace MATS and to indicate hot spots or hot moments [*McClain et al.*, 2003] of stream metabolic activity in transient storage zones. Questions remain, however, about Raz and Rru sorption, variability among different streams and ecosystems, decay, and abiotic transformation (if any). Further work is needed on these factors to help us constrain interpretation of field tracer results.

[37] Well data from this study together with lab column results from *Haggerty et al.* [2008] suggest a correlation of the transformation of Raz with aerobic respiration. In the hyporheic zone, both in the column and field experiments, F_{Raz} generally dropped with F_{O_2} (Figure 7). Similarly, F_{Rru} at first rose with falling F_{O_2} and then dropped. The initial rise is due to transformation of Raz to Rru and the later drop is due to decay of Rru. Field results were consistent with the lab results except that rates were lower in the lab than in the field (field: $k_1^s/k_{O_2}^s = 1.22$, $k_{12}^s/k_{O_2}^s = 4.44$, and $k_2^s/k_{O_2}^s = 8.61$; lab: $k_1^s/k_{O_2}^s = 0.35$, $k_{12}^s/k_{O_2}^s = 3.49$, and $k_2^s/k_{O_2}^s = 1.27$). The value of $k_{O_2}^s$ in the lab experiments was 0.40 h^{-1}, whereas it was 0.18 h^{-1} in the hyporheic zone during the field experiment. The higher lab values may be due to smaller average grain size (the column experiments had a maximum grain size of approximately 2 mm) and therefore larger surface area and possibly higher organic carbon (i.e., more bacteria) in fine sediment. The higher lab values may also be due to the warmer temperatures in the lab (16°C) than in the field (~9.5°C; Table 1).

[38] The Raz to Rru transformation and associated decay may occur at different rates in the surface and subsurface compartments of transient storage. To begin to investigate this, we sampled four pools in addition to the wells. The pool concentrations (Figure 3a) of Raz and Rru were higher than in the thalweg during the first longitudinal sampling (sunset, $t = 7$ h). However, the presence of higher Raz concentration was puzzling, because we were aware of no way for the pools to accumulate and retain Raz unless the higher Raz concentrations came from upstream. This offered the clue to the puzzle, because Raz concentrations were dropping in the time previous to $t = 7$ h (Figures 3c and 3d) but were approximately constant prior to $t = 18$ h. The most likely explanation for the higher Raz in the pools is that the pools were filled with water at higher Raz concentrations prior to sampling (at $t = 7$ h) and that water was retained. This supports previous findings from *Gooseff et al.* [2005], who found mean residence times in pools of a similar-sized stream to be 3.0 h, sufficiently long to cause the anomalous Raz concentrations found in pools. At $t = 7$ h, the average Raz concentration in the pools was 5.2 μg L^{-1} higher than in the thalweg. At S2 and S3, we found Raz concentrations approximately this much higher 3–4 h earlier (at $t = 4$–5 h). This suggests residence times in the pools of 3–4 h. Rru was also higher in the pools at $t = 7$ h, a fact that could be explained by reduction of Raz to Rru in the pools. *Haggerty et al.* [2008] measured Raz to Rru transformation in unfiltered water from Riera de Santa Fe and found $k_{12}^c = 9.89 \times 10^{-4}$ h^{-1}, which indicates that many hundreds of hours are required for significant Rru concentrations to be generated in the water column. This suggests that the transformation is localized in the benthic zone, where both autotrophic and heterotrophic processes can occur. However, it is unclear why, at the sunrise longitudinal sampling, Rru was not higher in the pools than in the main channel.

More studies will be necessary to parse MATS pools from MATS hyporheic zones.

[39] Spatial heterogeneity or temporal changes in metabolic activity (hot spots and moments) should appear as differences in Raz transformation to Rru both along the stream and over time. The BTCs (Figures 3c and 3d) display a number of subtle changes in C_{Raz} and C_{Rru} that are most easily seen by comparing to the model, which is smooth. For example, there was a marked rise in Raz after sunset at both S2 and S3, followed by a fall. Raz and Rru standards did not show this rise and fall, and the rise and fall were not present in the Cl data. These facts suggest that the rise and fall after sunset was probably related to a drop in instantaneous rates of NEP at sunset (Figure 5).

[40] Spatial heterogeneity in Raz and Rru is difficult to discern in the longitudinal profiles, though a plot of the longitudinal profiles together (not shown) does suggest subtle heterogeneity that is not present in the Cl data. Heterogeneity in Raz and Rru may be due to heterogeneity in MATS along the stream. The smallest scale at which variability in underlying processes is expected to be visible with the Raz tracer is determined by the surface water mixing length, typically 1 to tens of meters in low-order streams; in the case of Santa Fe, the mixing length was ~25 m due to relatively fast moving water. The lack of significant heterogeneity in the Raz and Rru profiles suggests that most heterogeneity in MATS was at scales smaller than 25 m.

[41] The tails in the BTCs after the solute addition was completed are consistent with our understanding of the three tracers. First, the Cl tail is consistent with moderate transient storage, dropping to approximately 6% of the plateau concentration 2 h after the injection ceased. Second, Raz had a steeper slope than either Cl or Rru, and Raz concentration reached background levels 2 h after the injection was stopped. Loss of the tail faster than the conservative tracer substantiates the transformation and decay of Raz in what we infer to be MATS. Once Raz enters MATS, it transforms to Rru and also decays to another, unknown, product. Third, the Rru tail was extensive. Two hours postinjection, Rru concentration was still 17% of the plateau concentration and still more than 50% of the initial postinjection (20 min after injection) tail concentration. This is a clear indication of slow release of Rru from the subsurface, the only storage zone with sufficient residence time to retain significant quantities of Rru for >2 h. The fact that the tail is significantly larger than the Cl tail is consistent with Rru being produced in the subsurface. Last, the BTC tails are consistent with the BTC fronts. In the BTC fronts, Raz rises rapidly, Cl moderately rapidly, and Rru has a broad shoulder that takes approximately 3 h to reach plateau.

[42] While the model results generally agree well with the experimental data, discrepancies suggest issues that we may not understand fully. We have already called attention to the temporal and spatial changes in C_{Raz} and C_{Rru}, which suggest temporal and spatial variability in transformation rates that are tied to temporal and spatial variability in metabolic activity. A different issue relates to the upstream boundary condition, which was 80 μg L^{-1} Raz in our model. However, the concentration in the carboy indicates that the upstream boundary should have been 107.7 μg L^{-1} Raz. Pool 1, 4.6 m downstream of the injection, had concentrations that are consistent with an injection concentration of 107.7 μg L^{-1} Raz. Though we injected 107.7 μg L^{-1}, the concentration must have quickly decayed to ~80 μg L^{-1} Raz. For this to have happened requires a very high Raz decay rate between the injection and first measurement point, i.e., in the 13 m between the injection and L1 (see map in Figure 1). The upper 13 m of the reach is not geomorphically distinct, but perhaps this section of the reach has higher metabolic activity. Alternatively, the injection had very high salt concentration (50,900 μg L^{-1}), which would have caused the injectate to sink. Prior to complete mixing, a disproportionate amount of the tracer may have been in contact with the streambed, or moved through the streambed. This would have generated higher rates of transformation and decay in the first few meters. This issue will require closer investigation in future injections.

[43] There was a mass loss (beyond the injection issue described above) of approximately 15%. In other words, the sum of Raz and Rru observed at S3 was approximately 15% lower than that observed at the most upstream location. The model captures this with the rate coefficients k_1 and k_2 (with both superscripts *s* and *c*) which are decay of Raz and Rru to other, unknown compounds. A small amount of this decay may have been due to photodegradation of Rru; most of this decay, however, was unidentified. We hypothesize that the unidentified decay is due to a combination of sorption that is irreversible on the timescale of the experiment and transformation of Raz and Rru to unknown compounds.

[44] The simple MATS model defined in equations (1)–(4) is a refinement of the TSM defined by *Bencala and Walters* [1983] and others [e.g., *Harvey et al.*, 1996; *Runkel*, 1998]. The exchange parameters t_s and A_s/A are the same as defined in the TSM. However, the estimated values of these parameters are likely different if measured with Raz and Rru than with Cl or another conservative tracer alone. Since Raz and Rru transform and decay preferentially in the MATS zones, the estimates of t_s and A_s/A obtained with the triple combination of Raz, Rru and Cl are an average of the values experienced by these three tracers. We hypothesize that MATS zones are a subset of all transient storage zones, but more work needs to be done before any conclusions about this can be drawn.

[45] MATS model parameters are reasonable and self-consistent. The parameter that most stands out is A_s/A, measured at 0.76. This is approximately three times larger than values previously measured at Santa Fe [*Argerich et al.*, 2008]. This discrepancy is not only due to Raz and Rru data, but also to the Cl tail being larger than previously observed tails. Previous work has found that transient storage parameters are scale-dependent [*Harvey and Wagner*, 2000; *Haggerty et al.*, 2002] and sensitive to the injection time [*Haggerty et al.*, 2004], particularly when an exponential residence time distribution is used. A multiday tracer test by *Dent et al.* [2007] showed a significantly larger hyporheic and parafluvial zone than could have been seen by a tracer test of a few hours duration. The larger value of A_s/A is consistent with the tracer test being 4.5 times longer than the tracer tests of *Argerich et al.* [2008].

[46] Use of Raz as a tracer may allow us to better predict the relationship between transient storage and nutrient retention. A key question is whether the Raz transformation

rate is correlated to rates of nutrient uptake. Rates of Raz transformation and decay at Santa Fe are similar to SRP uptake rates. On the basis of the model parameters, we calculated a Raz S_w, of 674 m, and a Raz V_f, of 0.69 mm min^{-1}. The Raz V_f was nearly identical to that for SRP, 0.70 mm min^{-1} [*von Schiller et al.*, 2008; *Argerich et al.*, 2008], but lower than that for NH_4 in the same reach (*von Schiller et al.*'s V_f for NH_4 was 3.4 ± 1.4 mm min^{-1} and *Argerich et al.*'s V_f for NH_4 was 2.2 ± 0.6 mm min^{-1}). If Raz is useful in predicting the relationship between transient storage and nutrient retention, we would expect future studies to show a correlation between V_f of Raz and that of nutrients.

6. Conclusions

[47] Results from the whole reach injection demonstrate the successful use of Raz in stream experiments and suggest that the Raz transformation to Rru may be used as a tracer of metabolic activity, specifically aerobic respiration, mostly associated with transient storage in small streams.

[48] The metabolically active transient storage (MATS) concept refines transient storage in a new way. Rather than organizing transient storage physically into hyporheic and dead zone exchange [e.g., *Gooseff et al.*, 2005], the MATS concept organizes transient storage functionally into metabolically similar storage zones that may be physically dissimilar (e.g., some pools and parts of the hyporheic zone with high respiration) and separates metabolically different storage zones though they may be physically similar (e.g., pools with and without significant respiration). This perspective follows calls for a functional definition of transient storage based on combined hydrologic and biogeochemical characteristics [*Findlay*, 1995; *Boulton et al.*, 1998; *Fisher et al.*, 1998; *Kemp et al.*, 2000].

[49] Results from this study indicate that it may be feasible to use Raz in streams to measure and study MATS, and that a standardized methodology to measure MATS could be adopted similar to what is commonly done with a conservative tracer (e.g., Cl) to measure transient storage. These results complement those obtained from the laboratory in a previous study [*Haggerty et al.*, 2008] and together indicate that Raz is a sensitive tracer that could help to add a metabolic characterization, aerobic respiration, to transient storage zone physical characterization. In this sense, the parameters derived from the MATS may help better explain the influence of transient storage on stream biogeochemical processing (e.g., nutrient retention).

[50] Finally, in this study we have developed a conceptual and a mathematical model that includes Raz transformation to Rru, transport in streams, and exchange with MATS. The MATS model, which uses first-order reactions, has been tested against the complex and multidimensional data set obtained from the field experiment. Results indicate that the MATS model reproduced the data reasonably well and provides parameter descriptors of the size of transient storage, the exchange between free-flowing water and transient storage zones, and the rate of Raz to Rru transformation in this zone.

[51] While results to date are promising, significant and important questions still remain about the Raz tracer test: (1) Does the correlation between aerobic respiration and Raz reduction hold in a range of systems? (2) Can we quantify MATS using Raz in a standardized manner across stream ecosystems? (3) Is Raz transformation a function of the community, if respiration is similar? (4) How do rates of Raz reduction differ among stream compartments (e.g., colonized sediment, benthic organic matter, epilithic biofilm)? (5) Why are the sum of Raz and Rru nonconservative in the field and what role does sorption versus reaction to currently unidentified compounds play? (6) Can parameters derived from the MATS model improve our understanding of the relationship between transient storage and stream nutrient retention?

Notation

A channel cross-sectional area [L^2].
A_s MATS zone cross-sectional area [L^2].
C_{Raz} concentration of Raz in the channel [ML^{-3}].
C_{Rru} concentration of Rru in the channel [ML^{-3}].
D dispersion coefficient [L^2T^{-1}].
F_{O_2} fraction of O_2 remaining, defined as the O_2 in the well divided by the O_2 that entered the hyporheic zone from the surface stream [dimensionless].
F_{Raz} fraction of Raz remaining, defined as the Raz concentration in the well divided by the Raz concentration that entered the hyporheic zone from the channel [dimensionless].
F_{Rru} fraction of Rru, defined as the Rru concentration in the well divided by the Rru concentration that entered the hyporheic zone from the channel [dimensionless].
k_1^c decay rate coefficient for Raz in the channel [T^{-1}].
k_1^s decay rate coefficient for Raz in the MATS zone [T^{-1}].
k_{12}^c transformation rate coefficient for Raz to Rru in the channel [T^{-1}].
k_{12}^s transformation rate coefficient for Raz to Rru in the MATS zone [T^{-1}].
k_2^c decay rate coefficient for Rru in the channel [T^{-1}].
k_{12}^s decay rate coefficient for Rru in the MATS zone [T^{-1}].
k_{1Tot}^s total loss rate for Raz in the MATS zone, defined as the sum of k_1^s and k_{12}^s [T^{-1}].
$k_{O_2}^s$ decay rate coefficient for O_2 in the MATS zone [T^{-1}].
M_{Raz} molecular weight of Raz [M mol^{-1}].
M_{Rru} molecular weight of Rru [M mol^{-1}].
Q discharge [L^3T^{-1}].
R_s retardation coefficient due to sorption in the MATS zone [dimensionless].
S_{Raz} concentration of Raz in the MATS zone [ML^{-3}].
S_{Rru} concentration of Rru in the MATS zone [ML^{-3}].
t time [T].
t_s mean residence time in the MATS zone for a conservative solute [T].
x distance from the injection point [L].
α exchange rate coefficient (for MATS zone) as defined in the transient storage literature [e.g., *Runkel*, 2007] [T^{-1}].
τ travel time from the stream surface to the well [T].

[52] **Acknowledgments.** We thank Miquel Ribot, Paula Fonollà, and Daniel Fernandez García for field assistance and Lynn Melton and Kim

Kangasniemi for tips on the Raz-Rru system. We are also grateful to the Direcció del Parc Natural del Montseny (Diputació de Barcelona) for ensuring access to the site during the experiment. We thank the Centre d'Estudis Avançats de Blanes (CSIC) for hosting R.H.'s and N.B.G.'s sabbatical where this work was primarily completed. This work was supported by sabbatical funding from the Ministerio de Educación y Ciencia of Spain and Oregon State University, by funding from the NICON (MEC, Spain, ref CGL2005–7362) and EUROLIMPACS (EC 6th Framework Program, ref GOCE-CT-2003-505540) projects, by STAMMT-L 3.0 code development from Sandia National Laboratories, and by support from the National Science Foundation (EAR 04-09534 and EAR 08-38338).

References

Argerich, A., E. Martí, F. Sabater, M. Ribot, D. von Schiller, and J. L. Riera (2008), Combined effects of leaf litter inputs and a flood on nutrient retention in a Mediterranean mountain stream during fall, *Limnol. Oceanogr.*, *53*(2), 631–641.

Bencala, K. E., and R. A. Walters (1983), Simulation of solute transport in a mountain pool-and-riffle stream: A transient storage model, *Water Resour. Res.*, *19*, 718–724, doi:10.1029/WR019i003p00718.

Bott, T. L. (2006), Primary productivity and community respiration, in *Methods in Stream Ecology*, 2nd ed., edited by F. R. Hauer and G. A. Lamberti, pp. 663–690, Academic, Paris.

Boulton, A. J., S. Findlay, P. Marmonier, E. H. Stanley, and H. M. Valett (1998), The functional significance of the hyporheic zone in streams and rivers, *Annu. Rev. Ecol. Syst.*, *29*, 59–81, doi:10.1146/annurev.ecolsys.29.1.59.

Bueno, C., M. L. Villegas, S. G. Bertolotti, C. M. Previtali, M. G. Neumann, and M. V. Encinas (2002), The excited-state interaction of resazurin and resorufin with amines in aqueous solutions, Photophysics and photochemical reaction, *Photochem. Photobiol.*, *76*(4), 385–390, doi:10.1562/0031-8655(2002)076<0385:TESIOR>2.0.CO;2.

Bukaveckas, P. A. (2007), Effects of channel restoration on water velocity, transient storage, and nutrient uptake in a channelized stream, *Environ. Sci. Technol.*, *41*, 1570–1576, doi:10.1021/es061618x.

Clesceri, L. S., A. E. Greenberg, and E. D. Eaton (1999), *Standard Methods for the Examination of Water and Wastewater*, 1325 pp., Am. Public Health Assoc., Washington, D. C.

Dahm, C. N., H. M. Valett, C. V. Baxter, and W. W. Woessner (2006), Hyporheic zones, in *Methods in Stream Ecology*, 2nd ed., edited by F. R. Hauer and G. A. Lamberti, pp. 119–142, Academic, Paris.

D'Angelo, D. J., J. R. Webster, S. V. Gregory, and J. L. Meyer (1993), Transient storage in Appalachian and Cascade mountain streams as related to hydraulic characteristics, *J. N. Am. Benthol. Soc.*, *12*(3), 223–235, doi:10.2307/1467457.

De Fries, R., and M. Mistuhashi (1995), Quantification of mitogen induced human lymphocyte proliferation: Comparison of Alamar Blue assay to 3H-thymidine incorporation assay, *J. Clin. Lab. Anal.*, *9*(2), 89–95, doi:10.1002/jcla.1860090203.

Dent, C. L., N. B. Grimm, E. Martí, J. W. Edmonds, J. C. Henry, and J. R. Welter (2007), Variability in surface-subsurface hydrologic interactions and implications for nutrient retention in an arid-land stream, *J. Geophys. Res.*, *112*, G04004, doi:10.1029/2007JG000467.

Findlay, S. (1995), Importance of surface-subsurface exchange in stream ecosystems: The hyporheic zone, *Limnol. Oceanogr.*, *40*, 159–164.

Fisher, S. G., N. B. Grimm, E. Martí, and R. Gómez (1998), Hierarchy, spatial configuration, and nutrient cycling in a desert stream, *Aust. J. Ecol.*, *23*(1), 41–52, doi:10.1111/j.1442-9993.1998.tb00704.x.

Gooseff, M. N., J. LaNier, R. Haggerty, and K. Kokkeler (2005), Determining in-channel (dead zone) transient storage by comparing solute transport in a bedrock channel–alluvial channel sequence, Oregon, *Water Resour. Res.*, *41*, W06014, doi:10.1029/2004WR003513.

Guerin, T. F., M. Mondido, B. McClenn, and B. Peasley (2001), Application of resazurin for estimating abundance of contaminant-degrading microorganisms, *Lett. Appl. Microbiol.*, *32*, 340–345, doi:10.1046/j.1472-765X.2001.00916.x.

Haggerty, R., and S. M. Gorelick (1995), Multiple-rate mass transfer for modeling diffusion and surface reactions in media with pore-scale heterogeneity, *Water Resour. Res.*, *31*, 2383–2400, doi:10.1029/95WR01583.

Haggerty, R., and P. Reeves (2002), STAMMT-L version 1.0 user's manual, 76 pp., Sandia Natl. Lab., Albuquerque, N. M.

Haggerty, R., S. M. Wondzell, and M. A. Johnson (2002), Power-law residence time distribution in the hyporheic zone of a 2nd-order mountain stream, *Geophys. Res. Lett.*, *29*(13), 1640, doi:10.1029/2002GL014743.

Haggerty, R., C. F. Harvey, C. F. von Schwerin, and L. C. Meigs (2004), What controls the apparent timescale of solute mass transfer in aquifers and soils? A comparison of diverse experimental results, *Water Resour. Res.*, *40*, W01510, doi:10.1029/2002WR001716.

Haggerty, R., A. Argerich, and E. Martí (2008), Development of a "smart" tracer for the assessment of microbiological activity and sediment-water interaction in natural waters: The resazurin-resorufin system, *Water Resour. Res.*, *44*, W00D01, doi:10.1029/2007WR006670.

Hall, R. O., Jr., E. S. Bernhardt, and G. E. Likens (2002), Relating nutrient uptake with transient storage in forested mountain streams, *Limnol. Oceanogr.*, *47*(1), 255–265.

Harvey, J. W., and K. E. Bencala (1993), The effect of streambed topography on surface-subsurface water exchange in mountain catchments, *Water Resour. Res.*, *29*, 89–98, doi:10.1029/92WR01960.

Harvey, J. W., and B. J. Wagner (2000), Quantifying hydrologic interactions between streams and their subsurface hyporheic zones, in *Streams and Ground Waters*, edited by J. B. Jones and P. J. Mulholland, pp. 3–44, Academic, San Diego, Calif.

Harvey, J. W., B. J. Wagner, and K. E. Bencala (1996), Evaluating the reliability of the stream tracer approach to characterize stream-subsurface water exchange, *Water Resour. Res.*, *32*, 2441–2451, doi:10.1029/96WR01268.

Johnson, S. L. (2004), Factors influencing stream temperatures in small streams: Substrate effects and a shading experiment, *Can. J. Fish. Aquat. Sci.*, *61*, 913–923, doi:10.1139/f04-040.

Kangasniemi, K. H. (2004), Fluorescent diagnostics for imaging dissolved oxygen, Ph.D. thesis, 62 pp., Univ. of Tex. at Dallas, Richardson.

Karakashev, D., D. Galabova, and I. Simeonov (2003), A simple and rapid test for differentiation of aerobic from anaerobic bacteria, *World J. Microbiol. Biotechnol.*, *19*, 233–238, doi:10.1023/A:1023674315047.

Kemp, J. L., D. M. Harper, and G. A. Crosa (2000), The habitat-scale ecohydraulics of rivers, *Ecol. Eng.*, *16*, 17–29, doi:10.1016/S0925-8574(00)00073-2.

Lautz, L. K., and D. I. Siegel (2007), The effect of transient storage on nitrate uptake lengths in streams: An inter-site comparison, *Hydrol. Process.*, *21*, 3533–3548, doi:10.1002/hyp.6569.

Liu, D. (1983), Resazurin reduction method for activated sludge process control, *Environ. Sci. Technol.*, *17*(7), 407–411, doi:10.1021/es00113a009.

Loheide, S., and S. Gorelick (2006), Quantifying stream-aquifer interactions through the analysis of remotely sensed thermographic profiles and in situ temperature histories, *Environ. Sci. Technol.*, *40*(10), 3336–3341, doi:10.1021/es0522074.

Losantos, M., E. Aragonès, X. Berástegui, J. Palau, C. Pugdefàbregas, and M. Soler (2002), *Mapa geològic de Catalunya*, 2nd ed., Inst. Cartogr. de Catalunya, Barcelona, Spain.

Mariscal, A., R. M. López-Gigosos, M. Carnero-Varo, and J. Fernández-Crehuet (2009), Fluorescent assay based on resazurin for detection of activity of disinfectants against bacterial biofilm, *Appl. Microbiol. Biotechnol.*, *82*, 773–783, doi:10.1007/s00253-009-1879-x.

Marquardt, D. (1963), An algorithm for least-squares estimation of nonlinear parameters, *SIAM J. Appl. Math.*, *11*, 431–441, doi:10.1137/0111030.

McClain, M. E., et al. (2003), Biogeochemical hot spots and hot moments at the interface of terrestrial and aquatic ecosystems, *Ecosystems*, *6*(4), 301–312, doi:10.1007/s10021-003-0161-9.

McNicholl, B. P., J. W. McGrath, and J. P. Quinn (2007), Development and application of a resazurin-based biomass activity test for activated sludge plant management, *Water Res.*, *41*, 127–133, doi:10.1016/j.watres.2006.10.002.

Mulholland, P. J., E. R. Marzolf, J. R. Webster, D. R. Hart, and S. P. Hendricks (1997), Evidence that hyporheic zones increase heterotrophic metabolism and phosphorus uptake in forest streams, *Limnol. Oceanogr.*, *42*(3), 443–451.

O'Brien, J., I. Wilson, T. Orton, and F. Pognan (2000), Investigation of the Alamar Blue (resazurin) fluorescent dye for the assessment of mammalian cell cytotoxicity, *Eur. J. Biochem.*, *267*, 5421–5426, doi:10.1046/j.1432-1327.2000.01606.x.

Peroni, C., and G. Rossi (1986), Determination of microbial activity in marine sediments by resazurin reduction, *Chem. Ecol.*, *2*(3), 205–218, doi:10.1080/02757548608080727.

Runkel, R. L. (1998), One-dimensional transport with inflow and storage (OTIS): A solute transport model for streams and rivers, *U.S. Geol. Surv. Water Resour. Invest. Rep., 98-4018*, 80 pp.

Runkel, R. L. (2007), Toward a transport-based analysis of nutrient spiraling and uptake in streams, *Limnol. Oceanogr. Methods*, *5*, 50–62.

Ryan, R. J., A. I. Packman, and S. S. Kilham (2007), Relating phosphorus uptake to changes in transient storage and streambed sediment characteristics in headwater tributaries of Valley Creek, an urbanizing watershed, *J. Hydrol. Amsterdam*, *336*, 444–457, doi:10.1016/j.jhydrol.2007.01.021.

Stream Solute Workshop (1990), Concepts and methods for assessing solute dynamics in stream ecosystems, *J. N. Am. Benthol. Soc.*, *9*, 95–119.

Sun, Y., and T. A. Buscheck (2003), Analytical solutions for reactive transport of N-member radionuclide chains in a single fracture, *J. Contam. Hydrol.*, *62–63*, 695–712, doi:10.1016/S0169-7722(02)00181-X.

Thomas, S. A., H. M. Valett, J. R. Webster, and P. J. Mulholland (2003), A regression approach to estimating reactive solute uptake in advective and transient storage zones of stream ecosystems, *Adv. Water Resour.*, *26*, 965–976, doi:10.1016/S0309-1708(03)00083-6.

Tizzard, A. C., J. H. Bergsma, and G. Lloyd-Jones (2006), A resazurin-based biosensor for organic pollutants, *Biosens. Bioelectron.*, *22*, 759–763, doi:10.1016/j.bios.2006.01.011.

Toride, N., F. J. Leij, and M. T. van Genuchten (1995), The CXTFIT code for estimating transport parameters from laboratory or field tracer experiments, version 2.0, research report, 121 pp., U.S. Salinity Lab., U.S. Dep. of Agric., Riverside, Calif.

Valett, H. M., J. A. Morrice, C. N. Dahm, and M. E. Campana (1996), Parent lithology, surface-groundwater exchange, and nitrate retention in headwater streams, *Limnol. Oceanogr.*, *41*, 333–345.

Valett, H. M., C. N. Dahm, M. E. Campana, J. A. Morrice, M. A. Baker, and C. S. Fellows (1997), Hydrologic influences on groundwater surface water ecotones: Heterogeneity in nutrient composition and retention, *J. N. Am. Benthol. Soc.*, *16*(1), 239–247, doi:10.2307/1468254.

von Schiller, D., E. Martí, J. L. Riera, M. Ribot, A. Argerich, P. Fonollà, and F. Sabater (2008), Inter-annual, annual, and seasonal variation of P and N retention in a perennial and an intermittent stream, *Ecosystems*, *11*(5), 670–687, doi:10.1007/s10021-008-9150-3.

Webster, J. R., et al. (2003), Factors affecting ammonium uptake in streams-an inter-biome perspective, *Freshwater Biol.*, *48*(8), 1329–1352, doi:10.1046/j.1365-2427.2003.01094.x.

Wörman, A., A. I. Packman, H. Johansson, and K. Jonsson (2002), Effect of flow-induced exchange in hyporheic zones on longitudinal transport of solutes in streams and rivers, *Water Resour. Res.*, *38*(1), 1001, doi:10.1029/2001WR000769.

Young, R. G., and A. D. Huryn (1996), Interannual variation in discharge controls ecosystem metabolism along a grassland river continuum, *Can. J. Fish. Aquat. Sci.*, *53*, 2199–2211, doi:10.1139/cjfas-53-10-2199.

A. Argerich, Departament d'Ecologia, Universitat de Barcelona, Diagonal 645, Barcelona E-08028, Spain. (alba@ceab.csic.es)

N. B. Grimm, Faculty of Ecology, Evolution and Environmental Science, School of Life Sciences, Arizona State University, 1711 South Rural Road, Tempe, AZ 85287-4501, USA. (nbgrimm@asu.edu)

R. Haggerty, Department of Geosciences, 104 Wilkinson Hall, Oregon State University, Corvallis, OR 97331-5506, USA. (haggertr@geo.oregonstate.edu)

E. Martí, Centre d'Estudis Avançats de Blanes, Consejo Superior de Investigaciones Científicas, Accés a la Cala St. Francesc 14, Blanes E-17300, Girona, Spain. (eugenia@ceab.csic.es)

D. von Schiller, Leibniz-Institute of Freshwater Ecology and Inland Fisheries, Müggelseedamm 310, D-12587 Berlin, Germany. (danielvonschiller@igb-berlin.de)